VIII International Conference on Computational Methods for Coupled Problems in Science and Engineering
COUPLED PROBLEMS 2019
E. Oñate, M. Papadrakakis and B. Schrefler (Eds)

AN ENERGY-MOMENTUM CONSISTENT TIME INTEGRATION SCHEME BASED ON A MIXED FRAMEWORK FOR NON-LINEAR ELECTRO-ELASTODYNAMICS

A. Janz*, M. Franke*, R. Ortigosa†, P. Betsch* and A.J. Gil††

* Institute of Mechanics, Karlsruhe Institute of Technology
76131 Karlsruhe, Germany
{alexander.janz, peter.betsch, marlon.franke}@kit.edu;
https://www.ifm.kit.edu/english/14.php

† Department of Applied Mathematics and Statistics, Polytechnic University of Cartagena
30203 Cartagena, Spain
rogelio.ortigosa@upct.es; https://personas.upct.es

†† Zienkiewicz Centre for Computational Engineering, College of Engineering, Swansea University, Bay Campus, SA1 8EN, United Kingdom a.j.gil@swansea.ac.uk;
http://www.swansea.ac.uk

Key words: Mixed variational framework, electroactive polymer, electro-elastodynamics, multi-variable convexity, energy-momentum scheme.

Abstract. The objective of the present work is the introduction of new mixed variational principles for EM time integrators in electromechanics, hence bridging the gap between the previous work presented by the authors in References [11] and [1], opening up the possibility to a variety of new Finite Element implementations.

1 Introduction

Dielectric elastomers represent an important family of Electro Active Polymers (EAPs) which are well-known for their outstanding actuation capabilities and low stiffness properties, which makes them ideal for their use as *soft robots*. Very recently, the authors in [11] proposed a new energy-momentum (EM in the sequel) preserving time integrator [15, 9, 14] for reversible electro-elastodynamics building upon [6]. As shown in [11], the new EM time integrator proved to be very robust and accurate for the long-term simulation of EAPs. The consistent implicit EM time integration scheme developed inherits the conservation laws of total energy,

linear momentum, angular momentum and electric charge. Specially relevant for the work carried out in this work is the recent work by Betsch et al. [1], where a new consistent EM time integration scheme has been developed in the context of polyconvex elasticity. In comparison to previously proposed discrete derivative expressions (see e.g. [9]), the new stress formula in [1, 6] assumes a remarkably simple form. A key factor for that simplification is the use of a tensor cross product pioneered by the Boer [4] and employed for the first time by Bonet et al. [2] in the case of nonlinear electromechanics [8, 13, 12]. Building upon the work presented in [11] and [1], the objective of this paper is to develop a new EM time integrator in the context of electro-elastodynamics based on a mixed variational formulation. The resulting new formulation opens up several possibilities in terms of its spatial discretisation and subsequent computational finite element implementation.

2 Nonlinear continuum electromechanics

A brief introduction into nonlinear continuum electromechanics and the relevant governing equations will be presented in this section.

2.1 Kinematics: motion and deformation

Let us consider the motion of an EAP with reference configuration $\mathcal{B}_0 \in \mathbb{R}^3$ and its boundary $\partial\mathcal{B}_0$ with unit outward normal $\boldsymbol{N}$. During its motion, the EAP occupies a deformed configuration $\mathcal{B} \in \mathbb{R}^3$ with boundary $\partial\mathcal{B}$ and unit outward normal $\boldsymbol{n}$. The motion of the EAP is defined by the mapping $\boldsymbol{\phi}(\boldsymbol{X}, t)$, which links a material particle from the reference configuration $\boldsymbol{X} \in \mathcal{B}_0$ to the deformed configuration $\boldsymbol{x} \in \mathcal{B}$ according to $\boldsymbol{x} = \boldsymbol{\phi}(\boldsymbol{X}, t)$. Associated with $\boldsymbol{\phi}(\boldsymbol{X}, t)$ it is possible to define the deformation gradient tensor $\boldsymbol{F}_{\boldsymbol{\phi}}$ [3] as

$$\boldsymbol{F}_{\boldsymbol{\phi}} = \boldsymbol{\nabla}_0 \boldsymbol{\phi}(\boldsymbol{X}, t); \qquad F_{\phi_{iI}} = \frac{\partial \phi_i}{\partial X_I}. \tag{1}$$

The deformation gradient tensor $\boldsymbol{F}_{\boldsymbol{\phi}}$[1] relates a fibre of differential length from the material configuration $d\boldsymbol{X}$ to the deformed configuration $d\boldsymbol{x} = \boldsymbol{F}_{\boldsymbol{\phi}} d\boldsymbol{X}$. In addition, differential area vector and volume elements in the reference configuration, $d\boldsymbol{A}$ (colinear with $\boldsymbol{N}$) and dV respectively, are mapped to the deformed configuration $d\boldsymbol{a}$ (colinear with $\boldsymbol{n}$) and dv, respectively, by means of the co-factor or adjoint tensor $\boldsymbol{H}_{\boldsymbol{\phi}}$ as $d\boldsymbol{a} = \boldsymbol{H}_{\boldsymbol{\phi}} d\boldsymbol{A}$ and the Jacobian $J_{\boldsymbol{\phi}}$ as $dv = J_{\boldsymbol{\phi}} dV$, respectively. Both $\boldsymbol{H}_{\boldsymbol{\phi}}$ and $J_{\boldsymbol{\phi}}$ can be related to $\boldsymbol{F}_{\boldsymbol{\phi}}$ as

$$\boldsymbol{H}_{\boldsymbol{\phi}} = (\det \boldsymbol{F}_{\boldsymbol{\phi}})\, \boldsymbol{F}_{\boldsymbol{\phi}}^{-T}; \qquad J_{\boldsymbol{\phi}} = \det \boldsymbol{F}_{\boldsymbol{\phi}}. \tag{2}$$

[1] Subscript $\boldsymbol{\phi}$ is included throughout the paper in order to emphasise the geometrically exact deformation term.

Equivalent expressions to those in (2) can be obtained by making use of the tensor cross product operation introduced by de Boer [4] and defined as

$$\boldsymbol{H}_{\boldsymbol{\phi}} = \frac{1}{2}\boldsymbol{F}_{\boldsymbol{\phi}} \times \boldsymbol{F}_{\boldsymbol{\phi}}; \qquad H_{\phi_{iI}} = \frac{1}{2}\mathcal{E}_{ijk}\mathcal{E}_{IJK}F_{\phi_{jJ}}F_{\phi_{kK}}; \tag{3a}$$

$$J_{\boldsymbol{\phi}} = \frac{1}{3}\boldsymbol{H}_{\boldsymbol{\phi}} : \boldsymbol{F}_{\boldsymbol{\phi}}; \qquad J_{\boldsymbol{\phi}} = \frac{1}{3}H_{\phi_{iI}}F_{\phi_{iI}}, \tag{3b}$$

where $\mathcal{E}_{ijk}$ (or $\mathcal{E}_{IJK}$) symbolises the third order alternating tensor components[2] and the use of repeated indices implies summation, unless otherwise stated.

2.2 Governing equations in nonlinear electromechanics: conservation of linear momentum and angular momentum

The local form of the balance of linear momentum [10] can be written as

$$\begin{aligned} \rho_0\dot{\boldsymbol{v}} - \mathrm{DIV}\left(\boldsymbol{F}_{\boldsymbol{\phi}}\boldsymbol{S}\right) - \boldsymbol{f}_0 &= \boldsymbol{0}; && \text{in } \mathcal{B}_0; \\ \left(\boldsymbol{F}_{\boldsymbol{\phi}}\boldsymbol{S}\right)\boldsymbol{N} &= \boldsymbol{t}_0; && \text{on } \partial_{\boldsymbol{t}}\mathcal{B}_0; \\ \boldsymbol{\phi} &= \bar{\boldsymbol{\phi}}; && \text{on } \partial_{\boldsymbol{\phi}}\mathcal{B}_0; \\ \boldsymbol{\phi}(t=0) &= \boldsymbol{\phi}_0; && \text{in } \mathcal{B}_0; \\ \boldsymbol{v}(t=0) &= \boldsymbol{v}_0; && \text{in } \mathcal{B}_0, \end{aligned} \tag{4}$$

where $\rho_0 : \mathcal{B}_0 \to \mathbb{R}^+$ represents the mass density of the EAP in the reference configuration, $\boldsymbol{v}$ the velocity field and $(\dot{\bullet})$ denotes differentiation with respect to time. $\boldsymbol{f}_0$ represents a body force per unit undeformed volume $\mathcal{B}_0$ and $\boldsymbol{t}_0$, the traction force per unit undeformed area applied on $\partial_{\boldsymbol{t}}\mathcal{B}_0 \subset \partial\mathcal{B}_0$, where $\partial_{\boldsymbol{t}}\mathcal{B}_0 \cup \partial_{\boldsymbol{\phi}}\mathcal{B}_0 = \partial\mathcal{B}_0$ and $\partial_{\boldsymbol{t}}\mathcal{B}_0 \cap \partial_{\boldsymbol{\phi}}\mathcal{B}_0 = \emptyset$. Furthermore, $\boldsymbol{\phi}_0$ and $\boldsymbol{v}_0$ denote the initial configuration and velocity, respectively. Finally, $\boldsymbol{S}$ represents the second Piola-Kirchhoff stress tensor and the local balance of angular momentum leads to the well-known tensor condition $\boldsymbol{S} = \boldsymbol{S}^T$. Note that $\boldsymbol{S}$ depends on the displacement and the electrical field and is comprised of unsymmetrical mechanical and an electrical contributions.

2.3 Governing equations in non-linear electromechanics: Gauss's and Faraday's laws

In the absence of magnetic and time dependent effects, Maxwell equations reduce to Gauss's and Faraday's laws. The local form of the Gauss' law can be written in a Lagrangian setting as

$$\begin{aligned} \mathrm{DIV}\boldsymbol{D}_0 - \rho_0^e &= 0; && \text{in } \mathcal{B}_0; \\ \boldsymbol{D}_0 \cdot \boldsymbol{N} &= -\omega_0^e; && \text{on } \partial_\omega\mathcal{B}_0, \end{aligned} \tag{5}$$

[2]Lower case indices $\{i, j, k\}$ will be used to represent the spatial configuration whereas capital case indices $\{I, J, K\}$ will be used to represent the material description.

where $\boldsymbol{D}_0$ is the Lagrangian electric displacement vector, ρ_0^e represents an electric volume charge per unit of undeformed volume $\mathcal{B}_0$ and ω_0^e, an electric surface charge per unit of undeformed area $\partial_\omega \mathcal{B}_0 \subset \partial \mathcal{B}_0$. Alternatively, the spatial electric displacement vector $\boldsymbol{D}$ can be obtained through the area push forward relationship $\boldsymbol{D}_0 = \boldsymbol{H}_{\boldsymbol{\phi}}^T \boldsymbol{D}$, [5]. The local form of the static Faraday's law can be written in a Lagrangian setting as

$$\begin{aligned} \boldsymbol{E}_0 &= -\boldsymbol{\nabla}_0 \varphi; && \text{in } \mathcal{B}_0; \\ \varphi &= \bar{\varphi}; && \text{on } \partial_\varphi \mathcal{B}_0, \end{aligned} \tag{6}$$

where $\boldsymbol{E}_0$ is the Lagrangian electric field vector and φ, the scalar electric potential. In (6), $\partial_\varphi \mathcal{B}_0$ represents the part of the boundary $\partial \mathcal{B}_0$ where essential electric potential boundary conditions are applied, where $\partial_\omega \mathcal{B}_0 \cup \partial_\varphi \mathcal{B}_0 = \partial \mathcal{B}_0$ and $\partial_\omega \mathcal{B}_0 \cap \partial_\varphi \mathcal{B}_0 = \emptyset$. The spatial electric field vector $\boldsymbol{E}$ can be obtained through the standard fibre transformation $\boldsymbol{E}_0 = \boldsymbol{F}_{\boldsymbol{\phi}}^T \boldsymbol{E}$ [5].

3 Electro-Elastodynamics

The objective of this section is to present the variational formulation that will be used in order to develop an EM time integration scheme in Section 4.

3.1 Extension to electro-elastodynamics

A point of departure is the following ten field action integral $L_{\widetilde{W}}$

$$\begin{aligned} L_{\widetilde{W}}\left(\boldsymbol{v}, \boldsymbol{\phi}, \varphi, \boldsymbol{D}_0, \boldsymbol{\mathcal{D}}, \boldsymbol{\Lambda}\right) &= \int_{t_0}^{t} \left(\int_{\mathcal{B}_0} \left(\dot{\boldsymbol{\phi}} - \frac{1}{2}\boldsymbol{v} \right) \cdot \rho_0 \boldsymbol{v} \, dV - \Pi_{\widetilde{W}}\left(\boldsymbol{\phi}, \varphi, \boldsymbol{D}_0, \boldsymbol{\mathcal{D}}, \boldsymbol{\Lambda}\right) \right) dt; \\ \Pi_{\widetilde{W}}\left(\boldsymbol{\phi}, \varphi, \boldsymbol{D}_0, \boldsymbol{\mathcal{D}}, \boldsymbol{\Lambda}\right) &= \int_{\mathcal{B}_0} \widetilde{W}\left(\boldsymbol{C}, \boldsymbol{G}, C, \boldsymbol{D}_0\right) \, dV + \int_{\mathcal{B}_0} \boldsymbol{D}_0 \cdot \boldsymbol{\nabla}_0 \varphi \, dV \\ &\quad + \int_{\mathcal{B}_0} \boldsymbol{\Lambda}_{\boldsymbol{C}} : \left(\boldsymbol{C}_{\boldsymbol{\phi}} - \boldsymbol{C}\right) \, dV + \int_{\mathcal{B}_0} \boldsymbol{\Lambda}_{\boldsymbol{G}} : \left(\frac{1}{2}\boldsymbol{C} \times \boldsymbol{C} - \boldsymbol{G} \right) dV \\ &\quad + \int_{\mathcal{B}_0} \Lambda_C \left(\frac{1}{3}\boldsymbol{C} : \boldsymbol{G} - C \right) dV - \Pi_{\text{ext}}^m\left(\boldsymbol{\phi}\right) - \Pi_{\text{ext}}^e\left(\varphi\right), \end{aligned} \tag{7}$$

where t_0 and t represent any two instances of time with $t > t_0$. Moreover, we introduce the sets $\boldsymbol{\mathcal{D}} = \{\boldsymbol{C}, \boldsymbol{G}, C\}$ and $\boldsymbol{\Lambda} = \{\boldsymbol{\Lambda}_{\boldsymbol{C}}, \boldsymbol{\Lambda}_{\boldsymbol{G}}, \Lambda_C\}$. Note that $\widetilde{W}$ denotes the internal energy expressed in terms of the extended symmetric mechanical kinematic set $\{\boldsymbol{C}_{\boldsymbol{\phi}}, \boldsymbol{G}_{\boldsymbol{\phi}}, C_{\boldsymbol{\phi}}\}$, defined as

$$\boldsymbol{C}_{\boldsymbol{\phi}} = \boldsymbol{F}_{\boldsymbol{\phi}}^T \boldsymbol{F}_{\boldsymbol{\phi}}; \qquad \boldsymbol{G}_{\boldsymbol{\phi}} = \frac{1}{2}\boldsymbol{C}_{\boldsymbol{\phi}} \times \boldsymbol{C}_{\boldsymbol{\phi}} = \boldsymbol{H}_{\boldsymbol{\phi}}^T \boldsymbol{H}_{\boldsymbol{\phi}}; \qquad C_{\boldsymbol{\phi}} = \frac{1}{3}\boldsymbol{G}_{\boldsymbol{\phi}} : \boldsymbol{C}_{\boldsymbol{\phi}} = J_{\boldsymbol{\phi}}^2, \tag{8}$$

and $\boldsymbol{D}_0$. See [8] and the references therein for details concerning material stability of reversible electro-elasticity problems. Furthermore, in (7) the external

contributions Π^m_{ext} and Π^e_{ext} are defined as

$$\Pi^m_{\text{ext}}(\boldsymbol{\phi}) = \int_{\mathcal{B}_0} \boldsymbol{f}_0 \cdot \boldsymbol{\phi}\, dV + \int_{\partial_{\boldsymbol{t}}\mathcal{B}_0} \boldsymbol{t}_0 \cdot \boldsymbol{\phi}\, dA; \qquad \Pi^e_{\text{ext}}(\varphi) = -\int_{\mathcal{B}_0} \rho^e_0 \varphi\, dV - \int_{\partial_\omega \mathcal{B}_0} \omega^e_0 \varphi\, dA. \tag{9}$$

Moreover, in (7) $\{\boldsymbol{v}, \boldsymbol{\phi}, \varphi, \boldsymbol{D}_0, \boldsymbol{\mathcal{D}}, \boldsymbol{\Lambda}\} \in \mathbb{V}^{\boldsymbol{\phi}} \times \mathbb{V}^{\boldsymbol{\phi}} \times \mathbb{V}^{\varphi} \times \mathbb{V}^{\boldsymbol{D}_0} \times \mathbb{V}^{\boldsymbol{\mathcal{D}}} \times \mathbb{V}^{\boldsymbol{\mathcal{D}}}$, with $\mathbb{V}^{\boldsymbol{\mathcal{D}}} = \mathbb{V}^{\boldsymbol{C}} \times \mathbb{V}^{\boldsymbol{G}} \times \mathbb{V}^{C}$, where

$$\begin{aligned}
\mathbb{V}^{\boldsymbol{\phi}} &= \left\{\boldsymbol{\phi} : \mathcal{B}_0 \to \mathbb{R}^3; \quad \boldsymbol{\phi} \in H^1(\mathcal{B}_0) \mid J_{\boldsymbol{\phi}} > 0,\ \boldsymbol{\phi} = \bar{\boldsymbol{\phi}} \text{ on } \partial_{\boldsymbol{\phi}}\mathcal{B}_0\right\};\\
\mathbb{V}^{\varphi} &= \left\{\varphi : \mathcal{B}_0 \to \mathbb{R}; \quad \varphi \in H^1(\mathcal{B}_0) \mid \varphi = \bar{\varphi} \text{ on } \partial_{\varphi}\mathcal{B}_0\right\};\\
\mathbb{V}^{\boldsymbol{D}_0} &= \left\{\boldsymbol{D}_0 : \mathcal{B}_0 \to \mathbb{R}^3;\ (\boldsymbol{D}_0)_I \in \mathbb{L}_2(\mathcal{B}_0)\right\}; \quad \mathbb{V}^{\boldsymbol{C}} = \left\{\boldsymbol{C} : \mathcal{B}_0 \to \mathbb{S};\ C_{IJ} \in \mathbb{L}_2(\mathcal{B}_0)\right\};\\
\mathbb{V}^{\boldsymbol{G}} &= \left\{\boldsymbol{G} : \mathcal{B}_0 \to \mathbb{S}; \quad G_{IJ} \in \mathbb{L}_2(\mathcal{B}_0)\right\}; \quad \mathbb{V}^{C} = \left\{C : \mathcal{B}_0 \to \mathbb{R};\ C \in \mathbb{L}_2(\mathcal{B}_0)\right\},
\end{aligned} \tag{10}$$

where H^1 denotes the Sobolev functional space of square integrable functions and derivatives, $\mathbb{L}_2$, the space of square integrable functions and $\mathbb{S}$, the space of symmetric second order tensors. By means of Hamilton's principle, the stationary conditions of $L_{\widetilde{W}}$ in (7) with respect to variations $\{\delta\boldsymbol{v}, \delta\boldsymbol{\phi}, \delta\varphi, \delta\boldsymbol{D}_0\}$ are

$$\begin{aligned}
\mathcal{W}_{\boldsymbol{v}} &= \int_{\mathcal{B}_0} \left(\boldsymbol{v} - \dot{\boldsymbol{\phi}}\right) \cdot \rho_0 \delta\boldsymbol{v}\, dV = 0;\\
\mathcal{W}_{\boldsymbol{\phi}} &= \int_{\mathcal{B}_0} \rho_0 \dot{\boldsymbol{v}} \cdot \delta\boldsymbol{\phi}\, dV + \int_{\mathcal{B}_0} \boldsymbol{\Lambda}_{\boldsymbol{C}} : D\boldsymbol{C}_{\boldsymbol{\phi}}[\delta\boldsymbol{\phi}]\, dV\\
&\qquad - \int_{\mathcal{B}_0} \boldsymbol{f}_0 \cdot \delta\boldsymbol{\phi}\, dV - \int_{\partial_{\boldsymbol{t}}\mathcal{B}_0} \boldsymbol{t}_0 \cdot \delta\boldsymbol{\phi}\, dA = 0;\\
\mathcal{W}_{\varphi} &= \int_{\mathcal{B}_0} \boldsymbol{D}_0 \cdot \boldsymbol{\nabla}_0 \delta\varphi\, dV + \int_{\mathcal{B}_0} \rho^e_0 \delta\varphi\, dV + \int_{\partial_\omega \mathcal{B}_0} \omega^e_0 \delta\varphi\, dA = 0;\\
\mathcal{W}_{\boldsymbol{D}_0} &= \int_{\mathcal{B}_0} \delta\boldsymbol{D}_0 \cdot \left(\partial_{\boldsymbol{D}_0}\widetilde{W} + \boldsymbol{\nabla}_0\varphi\right) dV = 0,
\end{aligned} \tag{11}$$

with the admissible variations defined as $\{\delta\boldsymbol{v}, \delta\boldsymbol{\phi}, \delta\varphi, \delta\boldsymbol{D}_0\} \in \mathbb{V}^{\boldsymbol{\phi}}_0 \times \mathbb{V}^{\varphi}_0 \times \mathbb{V}^{\boldsymbol{D}_0}$, being

$$\begin{aligned}
\mathbb{V}^{\boldsymbol{\phi}}_0 &= \left\{\boldsymbol{\phi} : \mathcal{B}_0 \to \mathbb{R}^3; \quad \boldsymbol{\phi} \in H^1(\mathcal{B}_0) \mid \boldsymbol{\phi} = \boldsymbol{0} \text{ on } \partial_{\boldsymbol{\phi}}\mathcal{B}_0\right\};\\
\mathbb{V}^{\varphi}_0 &= \left\{\varphi : \mathcal{B}_0 \to \mathbb{R}^3; \quad \varphi \in H^1(\mathcal{B}_0) \mid \varphi = 0 \text{ on } \partial_{\varphi}\mathcal{B}_0\right\}.
\end{aligned} \tag{12}$$

Note that integration by parts with respect to time has been used on the inertia term of $(11)_b$. Equation $(11)_a$ represents the weak form for the relationship between the velocity field $\boldsymbol{v}$ and the time derivative of the mapping $\boldsymbol{\phi}$ and equation $(11)_b$, the balance of linear momentum (4). Notice that in $(11)_b$, the Lagrange multiplier $\boldsymbol{\Lambda}_{\boldsymbol{C}}$ coincides in a weak sense with half of the second Piola-Kirchhoff stress tensor $\boldsymbol{S}$. Eventually, equations $(11)_c$ and $(11)_d$ represent the weak forms of the Gauss

(5) and Faraday (6) laws, respectively. The stationary conditions of $L_{\widetilde{W}}$ (7) with respect to variations $\delta\boldsymbol{\mathcal{D}}$ yield,

$$\begin{aligned}
\mathcal{W}_{\boldsymbol{C}} &= \int_{\mathcal{B}_0} \delta\boldsymbol{C} : \left(\partial_{\boldsymbol{C}}\widetilde{W} - \boldsymbol{\Lambda}_{\boldsymbol{C}} + \boldsymbol{\Lambda}_{\boldsymbol{G}} \boldsymbol{\times} \boldsymbol{C} + \frac{1}{3}\Lambda_C \boldsymbol{G} \right) dV = 0; \\
\mathcal{W}_{\boldsymbol{G}} &= \int_{\mathcal{B}_0} \delta\boldsymbol{G} : \left(\partial_{\boldsymbol{G}}\widetilde{W} - \boldsymbol{\Lambda}_{\boldsymbol{G}} + \frac{1}{3}\Lambda_C \boldsymbol{C} \right) dV = 0; \\
\mathcal{W}_{C} &= \int_{\mathcal{B}_0} \delta C \left(\partial_{C}\widetilde{W} - \Lambda_C \right) dV = 0,
\end{aligned} \tag{13}$$

with $\{\delta\boldsymbol{C}, \delta\boldsymbol{G}, \delta C\} \in \mathbb{V}^{\boldsymbol{C}} \times \mathbb{V}^{\boldsymbol{G}} \in \mathbb{V}^{C}$. Notice that equation (13) represents the weak form of the constitutive equations. Finally, the stationary conditions of $L_{\widetilde{W}}$ (7) with respect to $\delta\boldsymbol{\Lambda}$ are

$$\begin{aligned}
\mathcal{W}_{\boldsymbol{\Lambda}_{\boldsymbol{C}}} &= \int_{\mathcal{B}_0} \delta\boldsymbol{\Lambda}_{\boldsymbol{C}} : (\boldsymbol{C}_{\boldsymbol{\phi}} - \boldsymbol{C}) \, dV = 0; \\
\mathcal{W}_{\boldsymbol{\Lambda}_{\boldsymbol{G}}} &= \int_{\mathcal{B}_0} \delta\boldsymbol{\Lambda}_{\boldsymbol{G}} : \left(\frac{1}{2}\boldsymbol{C} \boldsymbol{\times} \boldsymbol{C} - \boldsymbol{G} \right) dV = 0; \\
\mathcal{W}_{\Lambda_C} &= \int_{\mathcal{B}_0} \delta\Lambda_C \left(\frac{1}{3}\boldsymbol{C} : \boldsymbol{G} - C \right) dV = 0,
\end{aligned} \tag{14}$$

with $\{\delta\boldsymbol{\Lambda}_{\boldsymbol{C}}, \delta\boldsymbol{\Lambda}_{\boldsymbol{G}}, \delta\Lambda_C\} \in \mathbb{V}^{\boldsymbol{C}} \times \mathbb{V}^{\boldsymbol{G}} \in \mathbb{V}^{C}$. It is worth emphasising that equation (14) represents the weak form of the kinematic constraints. This particular choice of kinematic constraints, taken from the EM time integrator presented by Betsch et. al. [1] in the context of elastodynamics, is crucial for the design of the EM time integration scheme in Section 4.

4 Energy-Momentum integration scheme for electro-elastodynamics

The objective of this section is to propose an EM preserving time discretisation scheme for the set of weak forms given in (11), (13) and (14). Let us consider a sequence of time steps $\{t_1, t_2, ..., t_n, t_{n+1}\}$, where t_{n+1} denotes the endpoint of the current time step. From the stationary conditions in (11), the following implicit one-step time integrator is proposed

$$\begin{aligned}
(\mathcal{W}_{\boldsymbol{v}})_{\text{algo}} &= \int_{\mathcal{B}_0} \left(\boldsymbol{v}_{n+1/2} - \frac{\Delta\boldsymbol{\phi}}{\Delta t} \right) \cdot \rho_0 \delta\boldsymbol{v} \, dV = 0; \\
(\mathcal{W}_{\boldsymbol{\phi}})_{\text{algo}} &= \int_{\mathcal{B}_0} \rho_0 \frac{\Delta\boldsymbol{v}}{\Delta t} \cdot \delta\boldsymbol{\phi} \, dV + \int_{\mathcal{B}_0} \boldsymbol{\Lambda}_{\boldsymbol{C}} : \left(D\boldsymbol{C}_{\boldsymbol{\phi}}[\delta\boldsymbol{\phi}] \right)_{\text{algo}} dV - \int_{\mathcal{B}_0} \boldsymbol{f}_{0_{n+1/2}} \cdot \delta\boldsymbol{\phi} \, dV \\
&\quad - \int_{\partial_{\boldsymbol{t}}\mathcal{B}_0} \boldsymbol{t}_{0_{n+1/2}} \cdot \delta\boldsymbol{\phi} \, dA = 0,
\end{aligned} \tag{15}$$

and

$$
\begin{aligned}
\left(\mathcal{W}_{\varphi}\right)_{\text{algo}} &= \int_{\mathcal{B}_0} \boldsymbol{D}_{0_{n+1/2}} \cdot \boldsymbol{\nabla}_0 \delta\varphi \, dV + \int_{\mathcal{B}_0} \rho^e_{0_{n+1/2}} \delta\varphi \, dV + \int_{\partial_\omega \mathcal{B}_0} \omega^e_{0_{n+1/2}} \delta\varphi \, dA = 0; \\
\left(\mathcal{W}_{\boldsymbol{D}_0}\right)_{\text{algo}} &= \int_{\mathcal{B}_0} \delta\boldsymbol{D}_0 \cdot \left(D_{\boldsymbol{D}_0} \widetilde{W} + \boldsymbol{\nabla}_0 \varphi_{n+1/2} \right) dV = 0.
\end{aligned}
\tag{16}
$$

Note that $\left(\mathcal{W}_{\boldsymbol{v}}\right)_{\text{algo}}$, $\left(\mathcal{W}_{\boldsymbol{\phi}}\right)_{\text{algo}}$, $\left(\mathcal{W}_{\varphi}\right)_{\text{algo}}$ and $\left(\mathcal{W}_{\boldsymbol{D}_0}\right)_{\text{algo}}$ in (15)-(16) represent the algorithmic or time discrete versions of the stationary conditions in (11) and $(\bullet)_{n+1/2} = \frac{1}{2}\left((\bullet)_{n+1} + (\bullet)_n\right)$ and $\Delta(\bullet) = (\bullet)_{n+1} - (\bullet)_n$. Furthermore the Lagrange multipliers $\boldsymbol{\Lambda}_{(\bullet)}$ are constant throughout the timestep, such that $\boldsymbol{\Lambda}_{(\bullet)} := \boldsymbol{\Lambda}_{(\bullet)_{n,n+1}}$. In equation $(15)_b$, where the algorithmic or time discrete directional derivative $(D\boldsymbol{C}_{\boldsymbol{\phi}}[\delta\boldsymbol{\phi}])^{\text{algo}}$ is defined as

$$
\left(D\boldsymbol{C}_{\boldsymbol{\phi}}[\delta\boldsymbol{\phi}]\right)_{\text{algo}} = \left(\left(\boldsymbol{\nabla}_0 \delta\boldsymbol{\phi}\right)^T \boldsymbol{F}_{\boldsymbol{\phi}_{n+1/2}} + \boldsymbol{F}^T_{\boldsymbol{\phi}_{n+1/2}} \boldsymbol{\nabla}_0 \delta\boldsymbol{\phi} \right). \tag{17}
$$

In addition, following [1], the algorithmic counterparts of the stationary conditions $\mathcal{W}_{\boldsymbol{C}}$, $\mathcal{W}_{\boldsymbol{G}}$ and $\mathcal{W}_C$ in (13) are

$$
\begin{aligned}
\left(\mathcal{W}_{\boldsymbol{C}}\right)_{\text{algo}} &= \int_{\mathcal{B}_0} \delta\boldsymbol{C} : \left(D_{\boldsymbol{C}} \widetilde{W} - \boldsymbol{\Lambda}_{\boldsymbol{C}} + \boldsymbol{\Lambda}_{\boldsymbol{G}} \boldsymbol{\times} \boldsymbol{C}_{n+1/2} + \frac{1}{3} \Lambda_C \boldsymbol{G}_{n+1/2} \right) dV = 0; \\
\left(\mathcal{W}_{\boldsymbol{G}}\right)_{\text{algo}} &= \int_{\mathcal{B}_0} \delta\boldsymbol{G} : \left(D_{\boldsymbol{G}} \widetilde{W} - \boldsymbol{\Lambda}_{\boldsymbol{G}} + \frac{1}{3} \Lambda_C \boldsymbol{C}_{n+1/2} \right) dV = 0; \\
\left(\mathcal{W}_{C}\right)_{\text{algo}} &= \int_{\mathcal{B}_0} \delta C \left(D_C \widetilde{W} - \Lambda_C \right) dV = 0.
\end{aligned}
\tag{18}
$$

Finally, following [1], the algorithmic counterpart of the stationary conditions $\mathcal{W}_{\boldsymbol{\Lambda}_{\boldsymbol{C}}}$, $\mathcal{W}_{\boldsymbol{\Lambda}_{\boldsymbol{G}}}$ and $\mathcal{W}_{\Lambda_C}$ (14) are

$$
\begin{aligned}
\left(\mathcal{W}_{\boldsymbol{\Lambda}_{\boldsymbol{C}}}\right)_{\text{algo}} &= \int_{\mathcal{B}_0} \delta\boldsymbol{\Lambda}_{\boldsymbol{C}} : \left(\boldsymbol{C}_{\boldsymbol{\phi}_{n+1}} - \boldsymbol{C}_{n+1} \right) dV = 0; \\
\left(\mathcal{W}_{\boldsymbol{\Lambda}_{\boldsymbol{G}}}\right)_{\text{algo}} &= \int_{\mathcal{B}_0} \delta\boldsymbol{\Lambda}_{\boldsymbol{G}} : \left(\frac{1}{2} \boldsymbol{C}_{n+1} \boldsymbol{\times} \boldsymbol{C}_{n+1} - \boldsymbol{G}_{n+1} \right) dV = 0; \\
\left(\mathcal{W}_{\Lambda_C}\right)_{\text{algo}} &= \int_{\mathcal{B}_0} \delta\Lambda_{\boldsymbol{C}} \left(\frac{1}{3} \boldsymbol{C}_{n+1} : \boldsymbol{G}_{n+1} - C_{n+1} \right) dV = 0.
\end{aligned}
\tag{19}
$$

In (15)-(16) and (18), $\{D_{\boldsymbol{C}}\widetilde{W}, D_{\boldsymbol{G}}\widetilde{W}, D_C\widetilde{W}, D_{\boldsymbol{D}_0}\widetilde{W}\}$ represent the discrete derivatives [9, 11, 6] of the internal energy $\widetilde{W}$ with respect to $\{\boldsymbol{C}, \boldsymbol{G}, C, \boldsymbol{D}_0\}$, respectively. In particular $\{D_{\boldsymbol{C}}\widetilde{W}, D_{\boldsymbol{G}}\widetilde{W}, D_C\widetilde{W}, D_{\boldsymbol{D}_0}\widetilde{W}\}$ are the algorithmic or time discrete counterparts of $\{\partial_{\boldsymbol{C}}\widetilde{W}, \partial_{\boldsymbol{G}}\widetilde{W}, \partial_C\widetilde{W}, \partial_{\boldsymbol{D}_0}\widetilde{W}\}$, respectively. The expressions for the

discrete derivatives $D_{\boldsymbol{C}}\widetilde{W}$, $D_{\boldsymbol{G}}\widetilde{W}$, $D_{C}\widetilde{W}$ and $D_{\boldsymbol{D}_0}\widetilde{W}$ in [11] comply also with the required conservation properties of the new time integrator in equations (15)-(16), (18) and (19). See [7] for details on the discrete derivatives and the consistent approximation of the balance laws for this time integrator.

5 Finite Element implementation

As standard in finite elements, the domain $\mathcal{B}_0$ described in Section 2.1 and representing the EAP is sub-divided into a finite set of non-overlapping elements $e \in \mathbb{E}$ such that

$$\mathcal{B}_0 \approx \mathcal{B}_0^h = \bigcup_{e\in\mathbb{E}} \mathcal{B}_0^e. \tag{20}$$

The unknown fields $\{\boldsymbol{v}, \boldsymbol{\phi}, \varphi, \boldsymbol{D}_0, \boldsymbol{\mathcal{D}}, \boldsymbol{\Lambda}_{\boldsymbol{\mathcal{D}}}\}$ in the semi-discrete weak forms $\{\mathcal{W}_{\boldsymbol{v}}, \mathcal{W}_{\boldsymbol{\phi}}, \mathcal{W}_{\varphi}, \mathcal{W}_{\boldsymbol{D}_0}\}$ in (15)-(16), $\mathcal{W}_{\boldsymbol{\mathcal{D}}}$ in (18) and $\mathcal{W}_{\Lambda_{\mathcal{D}}}$ in (19) are discretised employing the following functional spaces $\mathbb{V}^{\boldsymbol{\phi}^h} \times \mathbb{V}^{\boldsymbol{\phi}^h} \times \mathbb{V}^{\varphi^h} \times \mathbb{V}^{\boldsymbol{D}_0^h} \times \mathbb{V}^{\boldsymbol{\mathcal{D}}^h} \times \mathbb{V}^{\boldsymbol{\mathcal{D}}^h}$, with $\mathbb{V}^{\boldsymbol{\mathcal{D}}^h} = \{\mathbb{V}^{\boldsymbol{C}^h}, \mathbb{V}^{\boldsymbol{G}^h}, \mathbb{V}^{C^h}\}$ defined as

$$\begin{aligned}
\mathbb{V}^{\boldsymbol{\phi}^h} &= \{\boldsymbol{\phi} \in \mathbb{V}^{\boldsymbol{\phi}};\quad \boldsymbol{\phi}^h\big|_{\mathcal{B}_0^e} = \sum_{a=1}^{n_{\text{node}}^{\boldsymbol{\phi}}} N_a^{\boldsymbol{\phi}} \boldsymbol{\phi}_a \mid \boldsymbol{\phi}_a = \bar{\boldsymbol{\phi}}^h \text{ on } \partial_{\boldsymbol{\phi}}\mathcal{B}_0^h\};\\
\mathbb{V}^{\varphi^h} &= \{\varphi \in \mathbb{V}^{\varphi};\quad \varphi^h\big|_{\mathcal{B}_0^e} = \sum_{a=1}^{n_{\text{node}}^{\varphi}} N_a^{\varphi} \varphi_a \mid \varphi_a = \bar{\varphi}^h \text{ on } \partial_{\varphi}\mathcal{B}_0^h\};\\
\mathbb{V}^{\boldsymbol{D}_0^h} &= \{\boldsymbol{D}_0 \in \mathbb{V}^{\boldsymbol{D}_0};\quad \boldsymbol{D}_0^h\big|_{\mathcal{B}_0^e} = \sum_{a=1}^{n_{\text{node}}^{\boldsymbol{D}_0}} N_a^{\boldsymbol{D}_0} \boldsymbol{D}_{0_a}\};\\
\mathbb{V}^{\boldsymbol{\mathcal{D}}^h} &= \{\boldsymbol{\mathcal{D}} \in \mathbb{V}^{\boldsymbol{\mathcal{D}}};\quad \boldsymbol{\mathcal{D}}_0^h\big|_{\mathcal{B}_0^e} = \sum_{a=1}^{n_{\text{node}}^{\boldsymbol{\mathcal{D}}}} N_a^{\boldsymbol{\mathcal{D}}} \boldsymbol{\mathcal{D}}_a\},
\end{aligned} \tag{21}$$

where for any field $\boldsymbol{\mathcal{Y}} \in \{\boldsymbol{\phi}, \varphi, \boldsymbol{D}_0, \boldsymbol{\mathcal{D}}, \boldsymbol{\Lambda}_{\boldsymbol{\mathcal{D}}}\}$, $n_{\text{node}}^{\boldsymbol{\mathcal{Y}}}$ denotes the number of nodes per element of the discretisation associated with the field $\boldsymbol{\mathcal{Y}}$ and $N_a^{\boldsymbol{\mathcal{Y}}} : \mathcal{B}_0^e \to \mathbb{R}$, the a^{th} shape function used for the interpolation of $\boldsymbol{\mathcal{Y}}$. In addition, $\boldsymbol{\mathcal{Y}}_a$ represents the value of the field $\boldsymbol{\mathcal{Y}}$ at the a^{th} node of a given finite element. Similarly, following a Bubnov-Galerkin approach, the functional spaces for the virtual variations $\{\delta\boldsymbol{v}, \delta\boldsymbol{\phi}, \delta\varphi, \delta\boldsymbol{D}_0, \delta\boldsymbol{\mathcal{V}}, \delta\boldsymbol{\Lambda}_{\boldsymbol{\mathcal{D}}}\} \in \mathbb{V}_0^{\boldsymbol{\phi}^h} \times \mathbb{V}_0^{\boldsymbol{\phi}^h} \times \mathbb{V}_0^{\varphi^h} \times \mathbb{V}^{\boldsymbol{D}_0^h} \times \mathbb{V}^{\boldsymbol{\mathcal{D}}^h} \times \mathbb{V}^{\boldsymbol{\mathcal{D}}^h}$ are defined as

$$\mathbb{V}_0^{\boldsymbol{\phi}^h} = \left\{\forall \boldsymbol{\phi} \in \mathbb{V}^{\boldsymbol{\phi}^h};\quad \boldsymbol{\phi} = \boldsymbol{0} \text{ on } \partial_{\boldsymbol{\phi}}\mathcal{B}_0\right\};\quad \mathbb{V}_0^{\varphi^h} = \left\{\forall \varphi \in \mathbb{V}^{\varphi^h};\quad \varphi = 0 \text{ on } \partial_{\varphi}\mathcal{B}_0\right\}. \tag{22}$$

Even though the relation between the time derivative of $\boldsymbol{\phi}$ and the velocity field $\boldsymbol{v}$ is considered in a weak manner (refer to the weak form $\mathcal{W}_{\boldsymbol{v}}$ in $(15)_a$), the consideration of equal functional spaces for both fields, namely $\boldsymbol{\phi} \in \mathbb{V}^{\boldsymbol{\phi}^h}$ and $\boldsymbol{v} \in \mathbb{V}^{\boldsymbol{\phi}^h}$

enables to conclude that equation $(15)_a$ holds strongly at the discrete level, namely[3]

$$\frac{\Delta \boldsymbol{\phi}}{\Delta t} = \boldsymbol{v}_{n+1/2}. \tag{23}$$

Finally, in order to reduce the computational cost of the proposed formulation, a piecewise discontinuous interpolation of the fields $\{\boldsymbol{D}_0, \boldsymbol{C}, \boldsymbol{G}, C, \boldsymbol{\Lambda_C}, \boldsymbol{\Lambda_G}, \Lambda_C\}$ is followed. A standard static condensation procedure [13, 2] is used to condense out the degrees of freedom of the fields $\{\boldsymbol{D}_0, \boldsymbol{C}, \boldsymbol{G}, C, \boldsymbol{\Lambda_C}, \boldsymbol{\Lambda_G}, \Lambda_C\}$.

6 Numerical example

In the numerical examples the internal energy is split into a purely mechanical and a coupled electromechanical part: $\widetilde{W}(\boldsymbol{C}, \boldsymbol{G}, C, \boldsymbol{D}_0) = \widetilde{W}_m(\boldsymbol{C}, \boldsymbol{G}, C) + \widetilde{W}_{em}(\boldsymbol{C}, C, \boldsymbol{D}_0)$. Herein we focus on ideal dielectric elastomers modelled by

$$\widetilde{W}_{em}(\boldsymbol{C}, C, \boldsymbol{D}_0) = \frac{1}{2\varepsilon_r \varepsilon_0 C^{1/2}} \boldsymbol{D}_0 \cdot \boldsymbol{C}\boldsymbol{D}_0. \tag{24}$$

An isotropic behaviour is considered for the mechanical component $\widetilde{W}_m$. Specifically, a Mooney-Rivlin strain energy functional is used, defined as

$$\widetilde{W}_m^{MR}(\boldsymbol{C}, \boldsymbol{G}, C) = \frac{\mu_1}{2}(\mathrm{tr}\boldsymbol{C} - 3) + \frac{\mu_2}{2}(\mathrm{tr}\boldsymbol{G} - 3) - (\mu_1 + 2\mu_2)\ln C^{1/2} + \frac{\lambda}{2}\left(C^{1/2} - 1\right)^2. \tag{25}$$

The material parameters are $\mu_1 = 5 \times 10^4\,\mathrm{Pa}$, $\mu_2 = 1 \times 10^5\,\mathrm{Pa}$, $\lambda = 5 \times 10^5\,\mathrm{Pa}$, $\epsilon_0 = 8.854 \times 10^{-12}\,\mathrm{A^2\,s^4\,kg^{-1}\,m^{-3}}$, $\epsilon_r = 4$ with reference density of $\rho_0 = 1000\,\mathrm{kg\,m^{-3}}$. From a mechanically point of view the actuator is free in space, i.e. no mechanical Dirichlet conditions are imposed and the initial velocity is assumed to be $\boldsymbol{V}_0 = \boldsymbol{\omega} \times \boldsymbol{X}$, with $\boldsymbol{\omega} = [0, 0, 0.05]^T\,s^{-1}$. On the blue electrode, a constant value of $\phi = 0\,\mathrm{V}$ is applied. On the purple electrode a time dependent electrical surface charge ω_0^e is applied, where the time dependent function of ω_0^e is given by $\omega_0^e = 5 \cdot 10^{-3} \cdot \sin(\frac{0.5\,\pi}{0.4\,\mathrm{s}}\,t)$ for $t \leq 0.4\,\mathrm{s}$, $\omega_0^e = 5 \cdot 10^{-3}$ for $0.4\,\mathrm{s} < t \leq 3.0\,\mathrm{s}$, $\omega_0^e = 5 \cdot 10^{-3} \cdot \cos(\frac{0.5\,\pi}{3.4\,\mathrm{s} - 3.0\,\mathrm{s}}\,(t - 3\,\mathrm{s}))$ for $3.0\,\mathrm{s} < t \leq 3.4\,\mathrm{s}$ and $\omega_0^e = 0$ for $t > 3.4\,\mathrm{s}$. The geometry and boundary conditions of the H-shaped actuator are depicted in Fig. 1. Ten node quadratic/four node linear tetrahedron (*tet 10/4*) elements are used, where Quadratic continuous interpolation spaces $P2^C$ and linear discontinuuous interpolation spaces $P1^D$ are employed such that $\{\boldsymbol{\phi}, \Phi\} \in P2^C$ and $\{\boldsymbol{D}_0, \boldsymbol{\mathcal{D}}, \boldsymbol{\Lambda}\} \in P1^D$. A mesh comprised of 15013 *tet 10/4* elements with a total of 95776

[3]Notice that in the discrete setting, $(15)_a$ transforms into a mass matrix multiplied by the discrete vector version of $\frac{\Delta \boldsymbol{\phi}}{\Delta t} - \boldsymbol{v}_{n+1/2}$ equaling zero. For this to hold, given the positive definite nature of the mass matrix, the discrete vector version of $\frac{\Delta \boldsymbol{\phi}}{\Delta t} - \boldsymbol{v}_{n+1/2}$ must be zero. Thus, equation (23) holds at the nodes of the discretisation and thus, at the quadrature points.

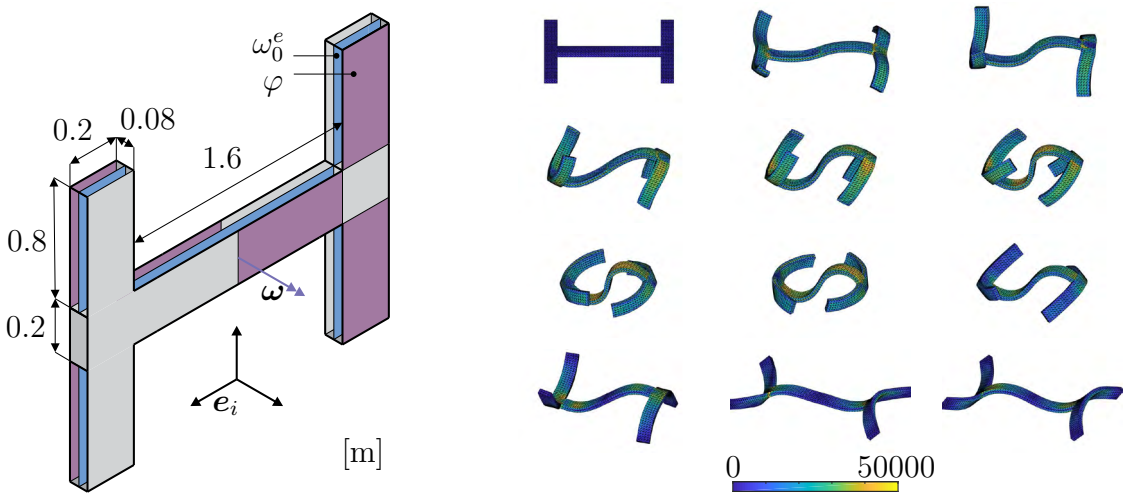

Figure 1: H-shaped actuator: Boundary conditions (left) and snapshots of the von Mises stress σ_{vM} for different configurations corresponding to $t = \{0, 0.4, 0.8, 1.2, 1.6, 2, 2.4, 2.8, 3.2, 3.6, 4, 4.4\}s$ (right).

displacement and electrical potential unknowns is employed. Fig. 1 shows typical snapshots of the H-shaped actuator displaying the von Mises stress σ_{vM} where extremely large deformations can be observed. Results are smooth and do not show any spurious pressure or electric field. Fig. 2 shows the evolution of the total Hamiltonian H and Fig. 3 the evolution of the norm of the total angular momentum $\boldsymbol{J}$ of the actuator for the proposed EM time integrator and the midpoint-rule. In addition, Fig. 2 shows that the midpoint-rule time integrator exhibits an energy blow-up and becomes unstable approximately in the interval $0.4\,s < t < 1.8\,s$. In contrast, the newly proposed EM time integrator perfectly conserves the energy after the loading phase. Also the discrete balance of angular momentum is perfectly preserved. The EM time integrator remains stable for the entire simulation time for the same fixed time step size of $\Delta t = 0.05\,s$. Accordingly, the proposed scheme is more robust and stable than the midpoint-rule.

See [7] for more numerical investigations demonstrating the beneficial spatial convergence behavior of the mixed formulation.

7 Conclusions

A new consistent energy-momentum one-step time integrator scheme is presented in the context of nonlinear electro-elastodynamics. The proposed schemes shows the typical advantages for the structure-preserving discretization in time. Furthermore, the mixed formulation offers several options for the discretization in space.

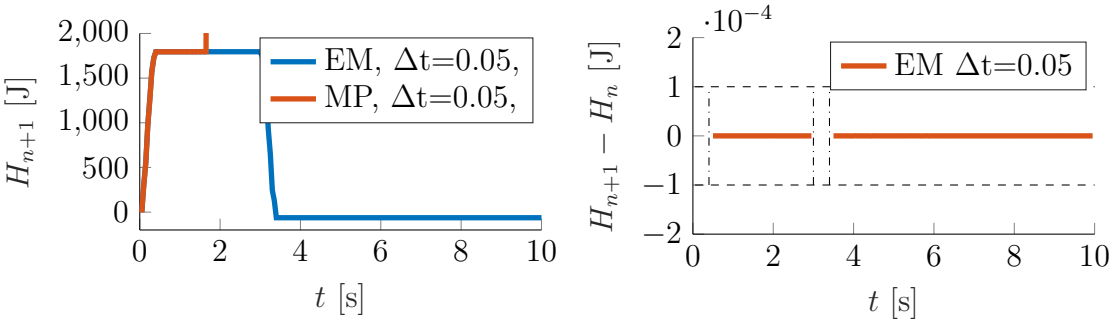

Figure 2: Left: Time evolution of H (left) and time evolution of ΔH (right).

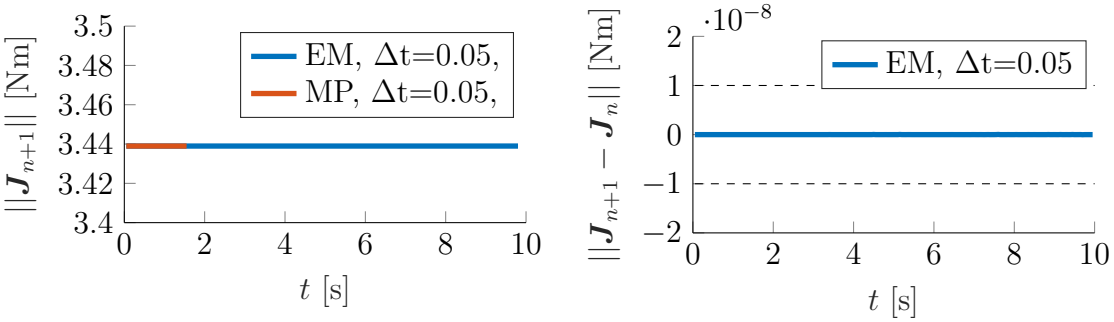

Figure 3: Time evolution of $||\boldsymbol{J}||$ (left) and time evolution of $\Delta||\boldsymbol{J}||$ (right).

REFERENCES

[1] P. Betsch, A. Janz, and C. Hesch. A mixed variational framework for the design of energy–momentum schemes inspired by the structure of polyconvex stored energy functions. *Computer Methods in Applied Mechanics and Engineering*, 335:660–696, 2018.

[2] J. Bonet, A. J. Gil, and R. Ortigosa. A computational framework for polyconvex large strain elasticity. *Computer Methods in Applied Mechanics and Engineering*, 283:1061–1094, 2015.

[3] J. Bonet, A. J. Gil, and R. D. Wood. *Nonlinear Continuum Mechanics for Finite Element Analysis: Statics*. Cambridge University Press, 2016.

[4] R. de Boer. *Vektor- und Tensorrechnung für Ingenieure*. Springer-Verlag, 1982.

[5] A. Dorfmann and R.W. Ogden. Nonlinear electroelastic deformations. *Journal of Elasticity*, 82(2):99–127, 2006.

[6] M. Franke, A. Janz, M. Schiebl, and P. Betsch. An energy momentum consistent integration scheme using a polyconvexity-based framework for nonlinear thermo-elastodynamics. *International Journal for Numerical Methods in Engineering*, 115(5):549–577, 2018.

[7] M. Franke, R. Ortigosa, A. Janz, A.J. Gil, and P. Betsch. A mixed variational framework for the design of energy-momentum integration schemes based on convex multi-variable electro-elastodynamics. *Computer Methods in Applied Mechanics and Engineering*, accepted for publication, 2019.

[8] A. J. Gil and R. Ortigosa. A new framework for large strain electromechanics based on convex multi-variable strain energies: variational formulation and material characterisation. *Computer Methods in Applied Mechanics and Engineering*, 302:293–328, 2016.

[9] O. Gonzalez. Exact energy and momentum conserving algorithms for general models in nonlinear elasticity. *Comput. Methods Appl. Mech. Engrg.*, 190:1763–1783, 2000.

[10] O. Gonzalez and A. M. Stuart. *A first course in Continuum Mechanics*. Cambridge University Press, 2008.

[11] R. Ortigosa, M. Franke, A. Janz, A.J. Gil, and P. Betsch. An energy-momentum time integration scheme based on a convex multi-variable framework for non-linear electro-elastodynamics. *Computer Methods in Applied Mechanics and Engineering*, 339:1–35, 2018.

[12] R. Ortigosa and A. J. Gil. A new framework for large strain electromechanics based on convex multi-variable strain energies: Conservation laws, hyperbolicity and extension to electro-magneto-mechanics. *Computer Methods in Applied Mechanics and Engineering*, 309:202–242, 2016.

[13] R. Ortigosa and A. J. Gil. A new framework for large strain electromechanics based on convex multi-variable strain energies: Finite element discretisation and computational implementation. *Computer Methods in Applied Mechanics and Engineering*, 302:329–360, 2016.

[14] I. Romero. An analysis of the stress formula for energy-momentum methods in nonlinear elastodynamics. *Computational Mechanics*, 50(5):603–610, Nov 2012.

[15] J. C. Simo and N. Tarnow. The discrete energy-momentum method. conserving algorithms for nonlinear elastodynamics. *Zeitschrift für angewandte Mathematik und Physik ZAMP*, 43(5):757–792, 1992.